AIP | Physics of Plasmas

Disruption avoidance in the SINP-Tokamak by means of electrode-biasing at the plasma edge

Debjyoti Basu, Rabindranath Pal, Julio J. Martinell, Joydeep Ghosh, and Prabal K. Chattopadhyay

Citation: Phys. Plasmas **20**, 052502 (2013); doi: 10.1063/1.4803656
View online: http://dx.doi.org/10.1063/1.4803656
View Table of Contents: http://pop.aip.org/resource/1/PHPAEN/v20/i5
Published by the American Institute of Physics.

Disruption avoidance in the SINP-Tokamak by means of electrode-biasing at the plasma edge

Debjyoti Basu,[1,2,a)] Rabindranath Pal,[1] Julio J. Martinell,[2] Joydeep Ghosh,[3] and Prabal K. Chattopadhyay[3]
[1]*Saha Institute of Nuclear Physics, 1/AF-Bidhannagar, Kolkata 700064, WB, India*
[2]*Instituto de Ciencias Nucleares-UNAM, Mexico D.F. 04510, Mexico*
[3]*Institute for Plasma Research, Gandhinagar, India*

(Received 28 January 2013; accepted 18 April 2013; published online 6 May 2013)

Control of plasma disruption by a biased edge electrode is reported in SINP-Tokamak. The features that characterize a plasma disruption are reduced with increasing bias potential. The disruption can be completely suppressed with the concomitant stabilization of observed MHD modes that are allegedly precursors of the disruption. An m = 3/n = 1 tearing mode, which apparently causes disruption can be stabilized when a negative biasing potential is applied near the edge. These changes in the disruptive behavior with edge biasing are hypothesized to be due to changes in the current density profile. © *2013 AIP Publishing LLC*. [http://dx.doi.org/10.1063/1.4803656]

INTRODUCTION

Plasma disruption[1,2] is a major issue for the stable operation of a tokamak due to its highly damaging effect and it should be avoided in large machines expected to attain the high confinement times needed for future fusion reactors. Major disruptions are mainly due to the growth of unstable MHD modes[3,4] or operation beyond the density limit[5,6] although the exact cause of this phenomenon is still an unsolved problem. Control of the large scale MHD instabilities, especially the $m = 2/n = 1$ and $m = 3/n = 2$ tearing modes is important to avoid disruptions. Different methods have been proposed and tested in several tokamaks to stabilize MHD modes, such as magnetic feedback stabilization,[7] injection of RF waves for electron cyclotron resonance heating (ECRH),[8] or electron cyclotron current drive (ECCD).[9,10] With ECRH and ECCD, conditions inside magnetic islands can be modified due to the small localization of wave deposition. FTU experiments[11] have shown the importance of MHD mode coupling for a disruption and used localized ECRH for disruption avoidance, by direct heating of magnetic islands which stops further growth and also produces the stabilization of the other modes. Current density redistribution can be achieved through ECRH and ECCD, which stabilizes the current-gradient-driven modes. Global change of current profile has been obtained by ECRH[8] and by ECCD.[9]

A series of detailed electrode biasing experiments in the SINP-Tokamak, whose main feature is that it can be operated from ultra low-q_a regime to high-q_a regime, showed that, over different q_a regimes, the current profile is modified as a result of the application of a fast $(\sim \mu s)$ biasing voltage at the plasma edge. Consequently, transport-producing drift modes in normal-q_a (Ref. 12) and $m = 2$ tearing mode in low-q_a (Ref. 13) have been stabilized, leading to improved plasma confinement. Local application of electric potential may thus lead to a global current profile change, which affects internal MHD modes. This assertion is supported by the observations reported here of the reduction of Mirnov probe oscillations and the stabilization of $m = 2/n = 1$ tearing mode and suppression of unstable $m = 3/n = 1$ tearing mode by applying a bias voltage. As a result, plasma disruptions have been controlled. This represents a simple experimental method supported by a physical picture, which might be extended to avoid disruptions in future tokamaks with the appropriate technology.

EXPERIMENTAL SETUP

The SINP-Tokamak is a small iron-core tokamak with $R = 30$ cm, $a = 7.5$ cm, and wall radius $a_w = 8.5$ cm. Detailed experimental description can be found in Ref. 12. In these experiments, plasma discharge duration is 10–15 ms. A highly purified cylindrically shaped tungsten electrode having 6 mm in diameter is inserted from the top port into the tokamak. The exposed length as well as electrode tip position have been kept fixed at 0.5 cm and $r = 6.7$ cm, respectively, for this experiment, where no plasma disturbances have been observed. A negative bias voltage was applied to the electrode with respect to the vacuum vessel from a 500 V, 500 A power supply that can be turned on in a time scale of tens of μs by a silicon-controlled rectifier (SCR) controlled fast trigger circuit. An important component is two sets of Mirnov probes that are used together with other diagnostics. These two sets are separated 90° toroidally. Each set consists of four Mirnov probes separated 90° poloidally. Multiple scans with reproducible results give confidence to our measurements.

ANALYSIS AND INTERPRETATION OF RESULTS

In the present experiment, plasma discharges are restricted to the normal q_a regime with $q_a \sim 5 - 7$. Very clean plasmas are used in almost all discharges to get steady and reproducible shots. All experimental scans start with a low −30 V bias voltage. Typical plasma parameters were $I_P = 18 - 23$ kA, $B_T = 1.2$ T, $T_e \approx 200$ eV, $n_e \approx (3 - 5) \times 10^{19}$ m^{-3}, and $q_a = 4.9$–6.2. Before the application of the biasing voltage,

a)Electronic address: debjyotibasu.basu@gmail.com

signatures of disruptions are found from loop voltage signals with dense negative spikes[14] at the falling stage of the plasma current in almost every shot. A typical disruption shot is shown in Fig. 1, where a hard disruption is seen at around 12 ms for the discharge represented with the light line. The negative loop voltage spike together with a positive spike in the plasma current is clearly seen.

The effect of the electrode biasing voltage on the disruption can be judged by comparing cases with and without bias under similar conditions. Fig. 1 shows that bias voltage suppresses the disruption. It is noticed that *soft* disruptions also appear in the case with bias at the falling stage of plasma current, coincident with the falling edge of bias voltage. The physical mechanism behind the disruption event should be determined and then elucidate how the application of a bias voltage helps to suppress it. Two of the main causes of disruptions are: unstable MHD disturbances and the attainment of a density limit. The second case can be ruled out in SINP tokamak since the Greenwald limit $n_G = 10^{20} I(MA)/(\pi a^2)\mathrm{m}^{-3} \sim 1.2 \times 10^{20}\,\mathrm{m}^{-3}$ is much higher that the nominal operating densities $n_e \sim (3-5) \times 10^{19}$. We then focus on the stability of magnetic disturbances.

First, the magnetic perturbations measured by the Mirnov probes are studied for the case without bias, in order to elucidate the features of the MHD modes related to disruptions. Examination of the time sequence of the signals shows that, typically, three time regions are present in the oscillations of each Mirnov coil which, in the typical shot of the present analysis (not the one in Fig. 1), are 3–5 ms, 5–9 ms, and 9–17 ms, extending from current flat-top to current termination. In the time region of 3–5 ms, no definite MHD mode is observed. But, in the time intervals of 5–9 ms and 9–17 ms characteristic MHD modes are present. First, the frequency power spectrum is obtained with FFT in the three time intervals and they are shown in Fig. 2. The first interval (Fig. 2(a)) is free from MHD activity, while the other two intervals show prominent peaks which determine the

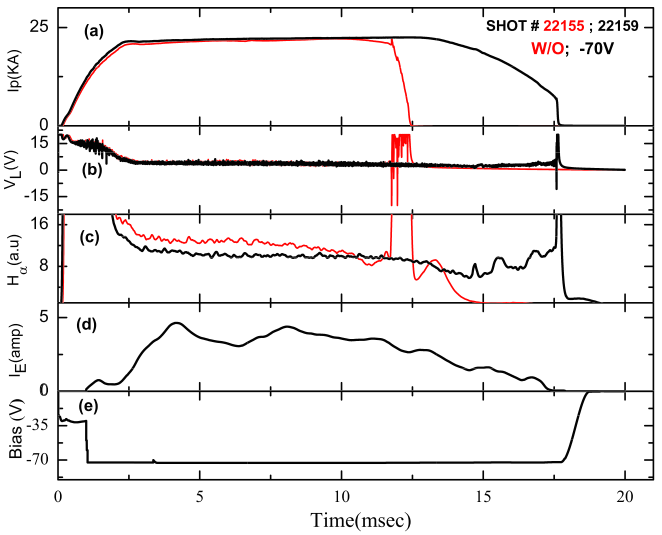

FIG. 1. Typical plasma discharge disruption. Temporal variation of (a) plasma current I_p, (b) loop voltage V_L, (c) intensity of H_α line, (d) electrode current, and (e) applied bias voltage. Without bias voltage (narrower line) and with bias voltage at −70 V (wider line).

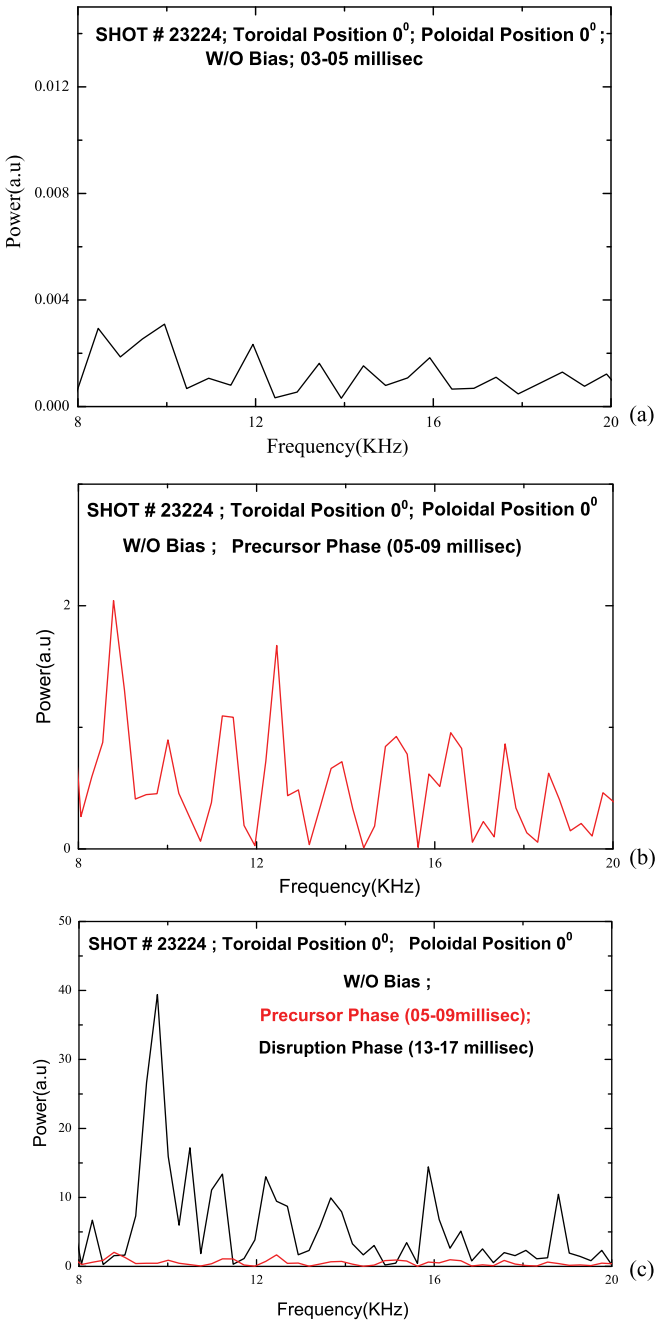

FIG. 2. Power spectra of typical Mirnov probe fluctuations at three phases: (a) pre-precursor phase (3–5 ms), (b) precursor phase (5–9 ms), and (c) disruption phase (13–17 ms) without bias. Precursor phase (lower power) is also shown in panel (c) for comparison.

dominant frequencies of the MHD modes. It is worth mentioning that these frequencies correspond to drift-tearing modes, which rotate at the observed frequency for some poloidal mode number m. To determine these numbers, relative phases of the four consecutive Mirnov oscillations are obtained following the conventional directions of the probes' locations. This has to be made with precaution due to the small number of coils available. We call the intervals 5–9 ms the disruption precursor phase (Fig. 2(b)) and 9–17 ms the disruption phase (Fig. 2(c)). Fig. 2 shows that the power level in the precursor phase is quite low compared to that in the disruption phase, which indicates that magnetic oscillations have grown strongly at the disruption time. This leads

to conclude that these are likely the main cause of the disruption.

During the precursor interval, there are two dominating frequency intervals at 12.5–13.2 kHz and 8.1–9.2 kHz seen in Fig. 2(b). These frequencies can be filtered from the actual time signal to determine the relative poloidal phases of consecutive Mirnov probes. These frequency-filtered signals are plotted in Figs. 3(a) and 3(b). The relative phase differences of consecutive Mirnov probe signals can be determined by looking at the vertical lines drawn to aid the eye. The signals for the frequency interval 12.5–13.2 kHz have an approximate phase difference of π between consecutive Mirnov coils, separated by $\pi/2$ which corresponds to poloidal mode number $m=2$, whereas for the range 8.1–9.2 kHz the phase difference is approximately $3\pi/2$, which corresponds to $m=3$. In order to better identify the mode numbers, in Fig. 3(c) we have plotted the phase difference of contiguous coils against the poloidal position of the coils for each frequency interval. Drawing a best fit straight line through the points, the mode number is obtained from the line slope. This analysis is facilitated in this case because the Mirnov coils are equally spaced and the plasma cross section is circular. When this is not the case, more elaborate analyses are required.[15,16] The fact that there are only four Mirnov coils leaves the possibility that there are mode nodes between coils which would produce a larger mode number, but we are assuming here that higher mode numbers are unlikely to be present and more difficult to detect. On the other hand, the toroidal mode number is indicated to be $n=1$ by looking at the relative phases between Mirnov coils at two toroidal positions 90° apart. We point out that, for both coil sets at the two toroidal positions, the relative poloidal phases are the same thus confirming that the determination of the m number is correct. The dominant tearing modes for the precursor ($m/n=2/1$ and 3/1) evolve as determined by the current profile, eventually leading to the disruption.

At the disruption time, a similar analysis reveals that there is a single dominant mode at frequency interval of 9–10 kHz, which is clearly observed in Fig. 2(c) for a representative coil. Form the frequency-filtered time signals for each of the four Mirnov coils, the relative phase differences can be determined and in Fig. 4 the plot of the signal phase vs poloidal angle is shown. From the slope of the best-fit line in this figure, it is clear that the mode number is $m=3$. Similarly, indication of toroidal mode number comes from the comparison of the two sets of toroidal coils; the frequency-filtered time signals at two toroidal positions for this case are shown in Fig. 5 and the relative phases indicate that $n=1$. The amplitude of this mode is almost one order of magnitude larger than those at the precursor phase and there is no clear evidence of an $m=2$ mode. This observation seems to imply that the growing mode $m/n=2/1$ couples with the outer $m/n=3/1$ mode, in the sense that the energy of the former is transferred to the latter stopping its growth, through some mechanism that we cannot determine with the available diagnostics. Possible causes are magnetic island overlap[4] or mode locking by resonant fields.[17] The unstable $m=3$ mode then leads to the disruption by connecting the confined plasma to the edge.

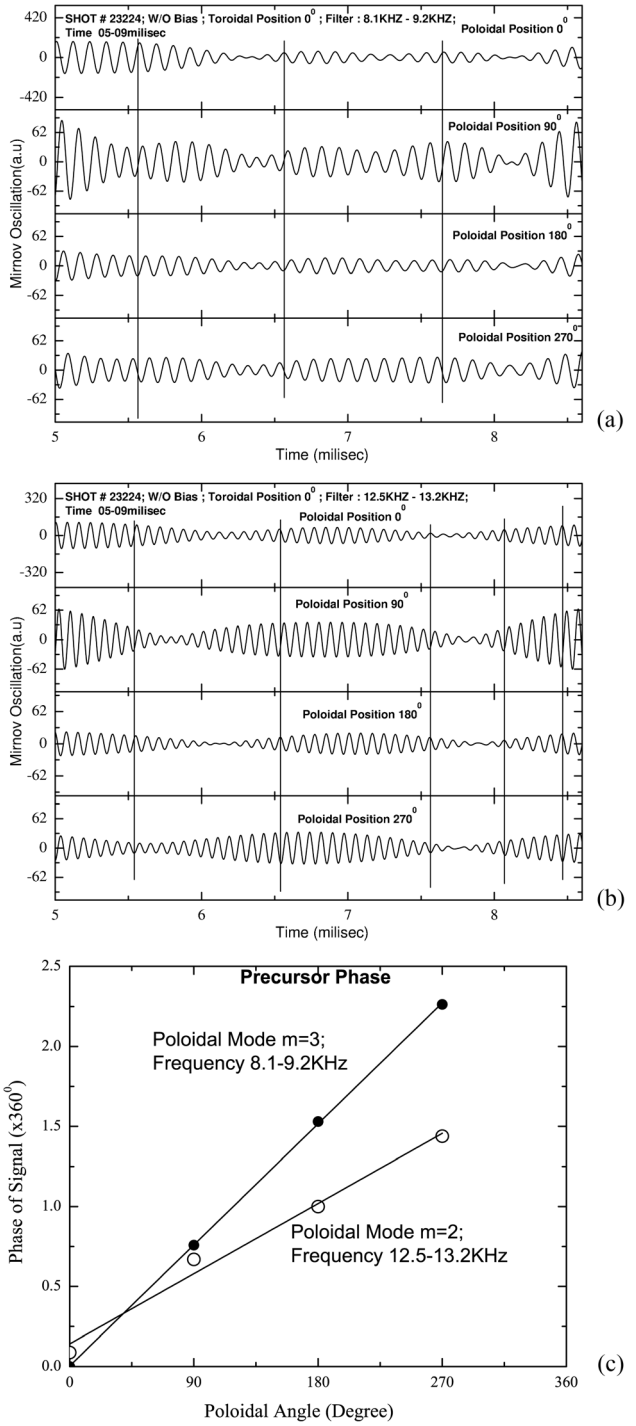

FIG. 3. Time evolution of frequency-filtered Mirnov coil signals at four poloidal locations in precursor phase (5–9 ms) with no bias. (a) Range 8.1–9.2 kHz indicates $m=3$ and (b) range 12.5–13.2 kHz indicates $m=2$ from spatial phase differences at same time instant (indicated by the vertical lines). (c) Mode numbers for cases (a) and (b) as the slope of the line that best fits the signal phases against the poloidal angle.

The presence of these modes can be checked to be consistent with the plasma parameters. For this, the temperature and current profiles are modeled to compute the rotation frequencies and compare with the experimental values. The electron temperature profile is taken as

$$T_e(r) = T_0[1-(r/a)^2]^p, \quad (1)$$

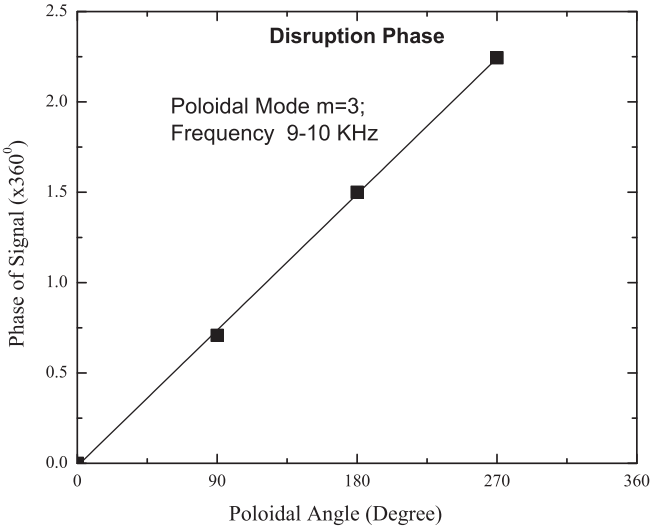

FIG. 4. Mirnov signal phase as a function of poloidal angle when filtered at frequency of 9–10 kHz in the disruption phase with no bias. The slope of the best-fit line indicates a mode number $m = 3$.

where p is determined from the experimental information as follows. For ohmic plasma, the current profile is obtained from the electrical conductivity as $J(r) \sim T_e(r)^{3/2}$ from which the $q(r)$ profile is found. Assuming that the observed frequency in the filtered Mirnov signals corresponds to the electron diamagnetic frequency $\omega_{*e} = cT_e/eB_TL_n$, the value of $T_e(r = r_m)$ at the $q(r = r_m) = m/n$ surface is derived (here $n = 1$) and from that the index p of the model profile. The density gradient scale length, L_n, used in ω_{*e} is estimated from a model density profile of the parabolic-like type $n = n_0[1 - (r/a)^2]^s$, with $s \approx 1.2$, and depending on the location of the mode it can be in the range $L_n \sim 1 - 4$ cm. The T_e profile obtained can then be used to find the frequency of other m-modes, and compare with the data. For the precursor phase, the central frequency of the $m = 2$ mode ($f \sim 12.8$ kHz) gives $p = 2.55$ and it is located at $r_2 = 0.58a$. With this profile index, radial positions for the modes $m = 3$ and $m = 5$ are obtained and the corresponding

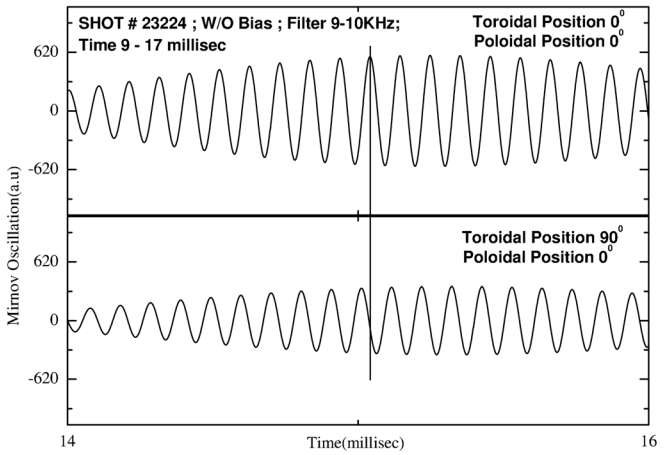

FIG. 5. Time evolution of frequency-filtered (9–10 kHz) Mirnov coil signals at two toroidal locations (90° apart) but in same poloidal locations (0°) in disruption phase with no bias indicates toroidal mode number $n = 1$ from spatial phase differences at same time instant (indicated by the vertical line).

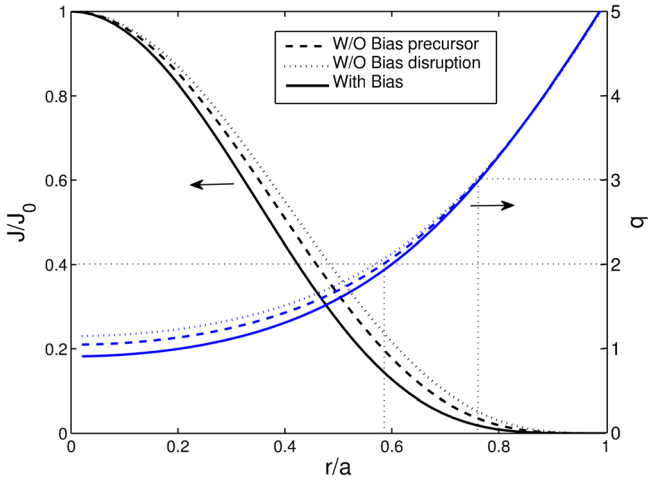

FIG. 6. Model radial profiles for normalized current density and q(r) in precursor (dashed line) and disruption (dotted line) phases with no bias and for biased case (continuous line), showing the location of q = 2, 3 surfaces for each case and corresponding current.

frequencies are $f \sim 8.7$ kHz and 15 kHz. This is exactly the observed frequency for the $m = 3$ mode and there is evidence for some smaller activity at the other frequency in Fig. 2(b), although the m-number for this mode could not be identified from the data due probably to some mode mixture. J/J_0 and q profiles for this phase are plotted in Fig. 6 with dashed lines. At the disruption stage, the same analysis is applied to the observed $m = 3$ mode giving $p = 2.34$ when the frequency $f \sim 9.5$ kHz of this mode is used, which is located at the radius $r_3 = 0.76a$. This profile is wider than the one at the precursor time and that produces a more unstable mode as it will be discussed in Discussion section. In Fig. 6, this is plotted with dotted lines.

Now consider a discharge with a biasing voltage applied at the plasma edge. In this case, the Mirnov oscillations have a very low amplitude but still provide information about the MHD modes. The relative power between the cases with and without bias can be seen in the power spectra of Fig. 7. Clearly, the MHD activity is drastically reduced when the bias voltage is applied. In Ref. 12, it was reported that

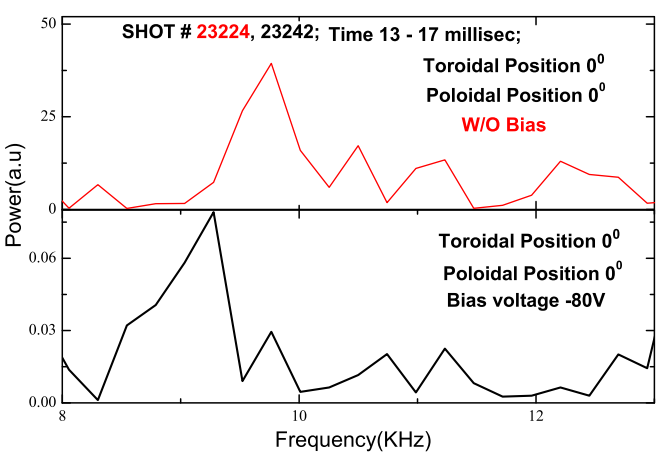

FIG. 7. Comparison of power spectra of typical Mirnov coil fluctuations in disruption phase (13–17 ms) with no bias (upper panel) and with −80 V bias (lower panel) for the same time interval. Notice the large difference in amplitudes of the peaks.

biasing experiments improve plasma confinement by stabilizing deleterious drift modes; in Fig. 2 of Ref. 12, the energy confinement time was shown to be improved for the same shots of Fig. 1. Current profile modification was reported in the outer plasma region, becoming steeper right inside the electrode position and this was associated to the improved confinement. The current redistribution should also affect current-driven tearing modes and hence a bias voltage would alter the ensuing disruption. The dominant mode in this case is at $f \sim 9-10$ kHz and Fig. 8 shows the oscillations at this frequency range for two different time intervals (corresponding to disruption stage 9–17 ms in the no bias case and to an extended interval 17–21 ms only present with the bias voltage). We point out that the signal amplitude does not change much up to the end of the plasma discharge, which indicates that there are no growing modes. The mode number is clearly identified as $m=2$, based on the analysis of Fig. 8 that gives the poloidal phase differences as before. The mode is present in both time intervals until the plasma discharge termination. Therefore, this mode does not grow and the other modes observed in the case with no bias are not excited, probably due to the current profile modification. This would prevent the mode coupling that led to the disruption when no bias was present.

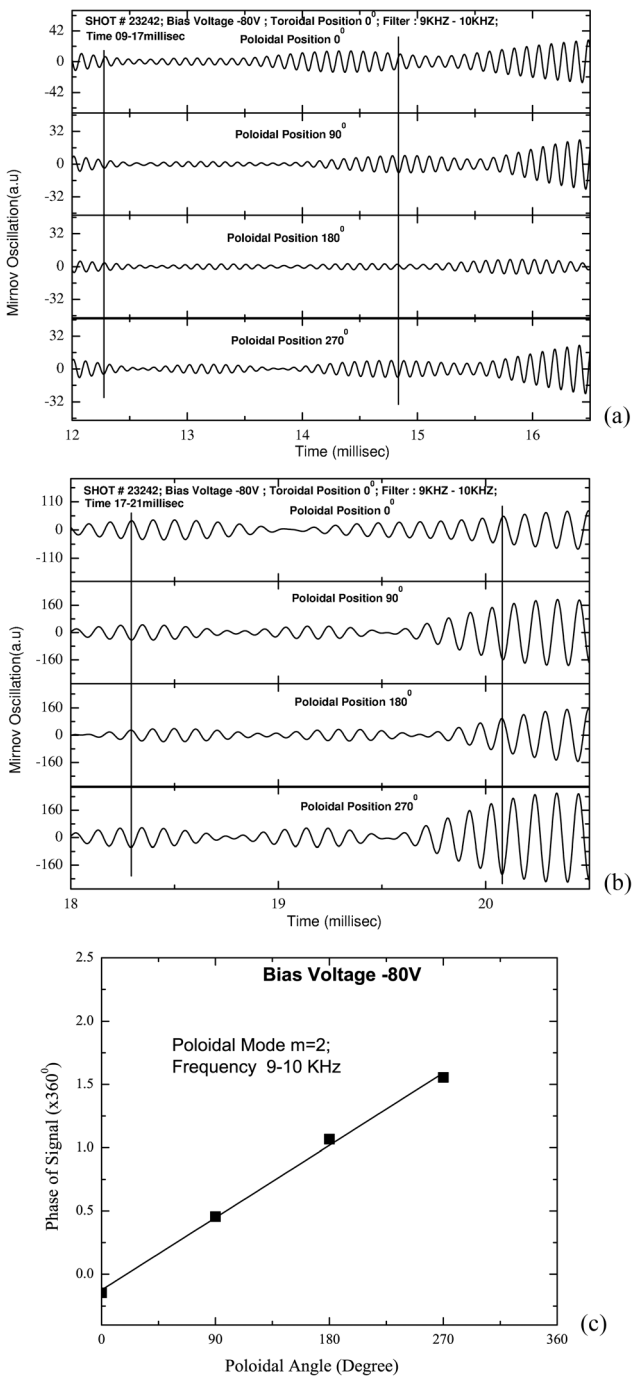

FIG. 8. Time evolution of frequency-filtered (9–10 kHz) Mirnov probes signals at four poloidal locations with −80 V bias at (a) time interval of 9–17 ms, coincident with disruption phase when there is no bias, (b) time interval of 17–21 ms (phase differences at vertical lines indicate that the poloidal mode number is $m=2$), and (c) plots the phases of the signals versus poloidal positions to get mode number through the slope of best fit line.

The same profile modeling as before can be made for this case, fitting Eq. (1) to the experimental profile using the frequency 9.5 kHz for $m=2$, giving $p=3.16$ with radial position $r_2 = 0.6a$. This corresponds to a narrower current profile compared with no biasing, in agreement with the observed current profile modification reported in Ref. 12. This is shown by the solid line in Fig. 6, which qualitatively agrees with the edge profile shape presented in Fig. 6(a) of Ref. 12, namely, steeper slope inside the electrode position. It is clear that this profile modeling does not prove the existence of the global current profile modification adduced above, but it provides a consistency check.

DISCUSSION

The analysis of the experimental results indicates that MHD modes get stabilized when electrode biasing is applied, which in turn avoids a plasma disruption. Specifically, without bias modes $m=2$ and 3 are unstable (although a coupling between them in the disruption phase makes $m=2$ mode imperceptible) and with bias $m=3$ is stable (is not excited) and $m=2$ is not growing (marginally stable). Based on previous results,[12,13] which show that electrode biasing produces current profile modification, it is proposed that the stabilization of tearing modes is due to changes in the current distribution. This hypothesis could be tested by computing the stability of the modes for a given current profile. One should bear in mind that the stability properties of tearing modes are very sensitive to the detailed profile shape and that experimental measurements of the current profile are not available, except for the edge region. Thus, reliable stability analysis cannot be done, but some insight can be gained if the model profiles from Eq. (1) are used. Following standard tearing mode stability analysis in cylindrical geometry,[18] the usual stability parameter Δ' has been computed by solving the mode equations for the model current profiles. The criterion for instability of mode m is that $\Delta' > 0$ at the position of the resonant surface $q=m$. The results give that, in general, mode $m=2$, which is located deeply inside the plasma column $(r/a \leq 0.6)$, is unstable while mode $m=3$, which is closer to the edge $(r/a \approx 0.76)$, is stable, for the profile parameters derived in last section $(2.3 < p < 3.2)$, although $m=3$ mode for profiles with no bias is close to marginal stability $(\Delta' = 0)$. Considering the approximate nature of the profiles,

one could say that $m=3$ is unstable without bias, which is consistent with the observations indicating that both $m=2$ and $m=3$ modes are unstable. In the case with bias, the profile change (which one should note from Fig. 6 that is not so large) produces a completely stable $m=3$ mode (now Δ' is convincingly negative) as the observations indicate; however, $m=2$ mode is still unstable. Clearly, the simple model profiles cannot account for the observed marginally stable mode, but it is likely that current gradients around the $q=2$ surface are different from those of the model profile.

To have an idea of how much the profile has to be changed to stabilize the modes, a scan of the profile parameter p was made. It was found that, for the range $1<p<4.6$ the mode $m=2$ was unstable and $m=3$ mode was stable. When $p>4.6$, both modes are stable. Thus, the current gradient corresponding to $p=4.6$ at $q=2$ should be locally produced by non-ideal effects; the smooth continuous line of Fig. 6 cannot account for a stable $m=2$ mode. But the model profiles were only intended to test the consistency of the observed frequencies. A more detailed stability analysis cannot be made with the available experimental information. Nevertheless, it is quite possible that the disruption is avoided because the current profile changes globally with biasing, which in turn prevents the development, growth, and coupling of tearing modes.

Another mechanism frequently mentioned for mode stabilization is the presence of poloidal plasma rotation due to the radial electric field at the electrode position. It is known that plasma rotation stops island growth due to the velocity shear, which produces a stabilizing perturbed polarization current which has an effect similar to mode locking.[19] However, we believe that this mechanism is not so important for SINP plasmas since the radial electric field is not present at all times in these discharges. In Fig. 7 of Ref. 12, it is shown that the radial electric field duration is short and it begins to decay just as mode formation begins, after 5 ms into the discharge.

The reason for the cancellation of the radial electric field while the toroidal current is modified is not completely clear but it may be due to the fact that the electrode intersects a magnetic island near the edge. Then, the negative electrode draws a parallel current which can bring charges from a different radial position in order to neutralize the ions collected at the electrode surface. This prevents the formation of a radial electric field while the parallel current has a radial component. As pointed out in Ref. 13, the parallel current can modify the toroidal current profile through nonlinear effects, as observed in the experiments.

CONCLUSIONS

The analysis presented here provides evidence that plasma disruption is avoided when negative electrode biasing is applied at the edge of the SINP-Tokamak, together with a drastic reduction of MHD activity. When no bias voltage is present, the detected modes that can be identified are $m/n=2/1$ and $m/n=3/1$, which apparently couple to leave only a large amplitude $m/n=3/1$ mode that leads to the disruption. These modes are stabilized by effect of negative biasing potential and only a steady $m/n=2/1$ mode is observed which is too far away from the plasma edge to produce a disruption. Based on previous analyses that indicate that the *edge* current density profile is modified when fast electrode bias is applied,[12] we hypothesize that the most likely cause of MHD modes' stabilization is the current profile modification. Calculation of *global* current profiles based on the observed frequencies also indicates that the profile is narrower with bias, which supports the assertion. Stability calculations of tearing modes for these model current profiles are consistent with the observed stabilization of the $m=3$ mode, but steeper profiles *locally* would be necessary to stabilize $m=2$ mode. The stabilized MHD modes allow to have a prolonged discharge relative to the case without bias. Disruption avoidance related to electrode bias has been, to our knowledge, first observed in SINP-Tokamak.

ACKNOWLEDGMENTS

We acknowledge discussions with C. Hidalgo and M. A. Pedrosa of CIEMAT, Spain. We thank all members of the Plasma Physics Group of Saha Institute of Nuclear Physics for generous help. This work was supported by a grant from DAE, Government of India. D.B. and J.J.M. acknowledge support from project PAPIIT IN106911 and a post-doctoral fellowship at UNAM and from project Conacyt 152905.

[1]T. C. Hender, J. C. Wesley, J. Bialek, A. Bondeson, A. H. Boozer, R. J. Buttery, A. Garofalo, T. P. Goodman, R. S. Granetz, Y. Gribov, O. Gruber, M. Gryaznevich, G. Giruzzi, S. Gnter, N. Hayashi, P. Helander, C. C. Hegna, D. F. Howell, D. A. Humphreys, G. T. A. Huysmans, A. W. Hyatt, A. Isayama, S. C. Jardin, Y. Kawano, A. Kellman, C. Kessel, H. R. Koslowski, R. J. La Haye, E. Lazzaro, Y. Q. Liu, V. Lukash, J. Manickam, S. Medvedev, V. Mertens, S. V. Mirnov, Y. Nakamura, G. Navratil, M. Okabayashi, T. Ozeki, R. Paccagnella, G. Pautasso, F. Porcelli, V. D. Pustovitov, V. Riccardo, M. Sato, O. Sauter, M. J. Schaffer, M. Shimada, P. Sonato, E. J. Strait, M. Sugihara, M. Takechi, A. D. Turnbull, E. Westerhof, D. G. Whyte, R. Yoshino, H. Zohm, and ITPA MHD, Disruption and Magnetic Control Topical Group, Nucl. Fusion **47**, S128 (2007).
[2]M. Sugihara, M. Shimada, H. Fujieda, Yu. Gribov, K. Ioki, Y. Kawano, R. Khayrutdinov, V. Lukash, and J. Ohmori, Nucl. Fusion **47**, 337 (2007).
[3]A. Sykes and J. A. Wesson, Phys. Rev. Lett. **44**, 1215 (1980).
[4]B. A. Carreras, H. R. Hicks, J. A. Holmes, and B. V. Waddell, Phys. Fluids **23**, 1811 (1980).
[5]R. G. Kleva and J. F. Drake, Phys. Fluids B **3**, 372 (1991).
[6]W. Suttrop, K. Buchl, J. C. Fuchs, M. Kaufmann, K. Lackner, M. Maraschek, V. Mertens, R. Neu, M. Schittenhelm, M. Sokoll, and H. Zohm, Nucl. Fusion **37**, 119 (1997).
[7]A. W. Morris, T. C. Hender, J. Hugill, P. S. Haynes, P. C. Johnson, B. Lloyd, D. C. Robinson, and C. Silvester, Phys. Rev. Lett. **64**, 1254 (1990).
[8]K. Hoshino, M. Mori, T. Yamamoto, H. Tamai, T. Shoji, Y. Miura, H. Aikawa, S. Kasai, T. Kawakami, H. Kawashima, M. Maeno, T. Matsuda, K. Oasa, K. Odajima, H. Ogawa, T. Ogawa, T. Seike, T. Shiina, K. Uehara, T. Yamauchi, N. Suzuki, and H. Maeda, Phys. Rev. Lett. **69**, 2208 (1992).
[9]C. C. Petty, R. J. La Haye, T. C. Luce, D. A. Humphreys, A. W. Hyatt, J. Lohr, R. Prater, E. J. Strait, and M. R. Wade, Nucl. Fusion **44**, 243 (2004).
[10]A. Isayama, G. Matsunaga, T. Kobayashi, S. Moriyama, N. Oyama, Y. Sakamoto, T. Suzuki, H. Urano, N. Hayashi, Y. Kamada, T. Ozeki, Y. Hirano, L. Urso, H. Zohm, M. Maraschek, J. Hobirk, K. Nagasaki, and JT-60 Team, Nucl. Fusion **49**, 055006 (2009).
[11]B. Esposito, G. Granucci, P. Smeulders, S. Nowak, J. R. Martn-Sols, L. Gabellieri, and FTU and ECRH Teams, Phys. Rev. Lett. **100**, 045006 (2008).

[12]D. Basu, R. Pal, J. Ghosh, and P. Chattopadhyay, Phys. Plasmas **19**, 072510 (2012).
[13]J. Ghosh, R. Pal, P. K. Chattopadhyay, and D. Basu, Nucl. Fusion **47**, 331 (2007).
[14]J. A. Wesson, D. J. Ward, and M. N. Rosenbluth, Nucl. Fusion **30**, 1011 (1990).
[15]M. Schittenhelm and H. Zohm, Nucl. Fusion **37**, 1255 (1997).
[16]J. S. Kim, D. H. Edgell, J. M. Greene, E. J. Strait, and M. S. Chance, Plasma Phys. Controlled Fusion **41**, 1399 (1999).
[17]S. M. Wolfe, I. H. Hutchinson, R. S. Granetz, J. Rice, A. Hubbard, A. Lynn, P. Phillips, T. C. Hender, D. F. Howell, R. J. La Haye, and J. T. Scoville, Phys. Plasmas **12**, 056110 (2005).
[18]H. P. Furth, P. H. Rutherford, and H. Selberg, Phys. Fluids **16**, 1054 (1973).
[19]T. C. Hender, R. Fitzpatrick, A. W. Morris, P. G. Carolan, R. D. Durst, T. Edlington, J. Ferreira, S. J. Fielding, P. S. Haynes, J. Hugill, I. J. Jenkins, R. J. La Haye, B. J. Parham, D. C. Robinson, T. N. Todd, M. Valovic, and G. Vayakis, Nucl. Fusion **32**, 2091 (1992).